Electronic Supplementary Material (ESI) for Environmental Science: Atmospheres.

Wavelength-resolved quantum yields for Vanillin Photochemistry: Self-Reaction and Ionic-Strength Implications for Atmospheric Brown Carbon Lifetime

Greg T. Drozd, Tate Weltzin, Sam Skiffington, Dong Lee, Rashid Valiev, Theo Kurtén, Lindsey R. Madison, Yiheng He, Lydia Gargano

Supplemental Information

Supplemental Figures

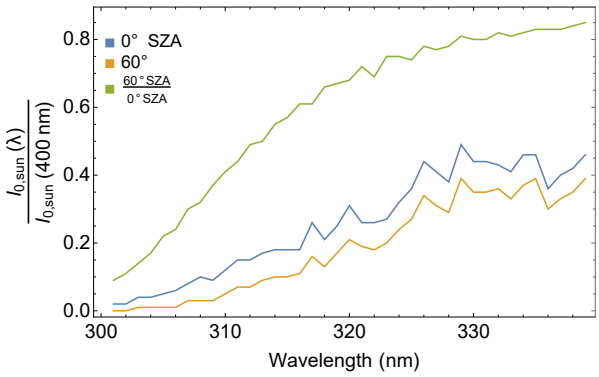

Figure S1. $I_{0,sun}(\lambda)$ *for 0 and 60° SZA, blue and yellow respectively, normalized to the solar intensity at 400nm for that SZA,* $I_{0,sun}(400nm)$. The green line shows the ratio of the normalized $I_{0,sun}(\lambda)$ at *60° SZA to that of 0° SZA, showing for example that* $I_{0,60°\,SZA}(311nm)/I_{0,60°\,SZA}(400)$ *has a value that is 1/2 that of the ratio* $I_{0,0°\,SZA}(311nm)/I_{0,0°\,SZA}(400)$. *Solar intensity data obtained from the NCAR TUV Model.*

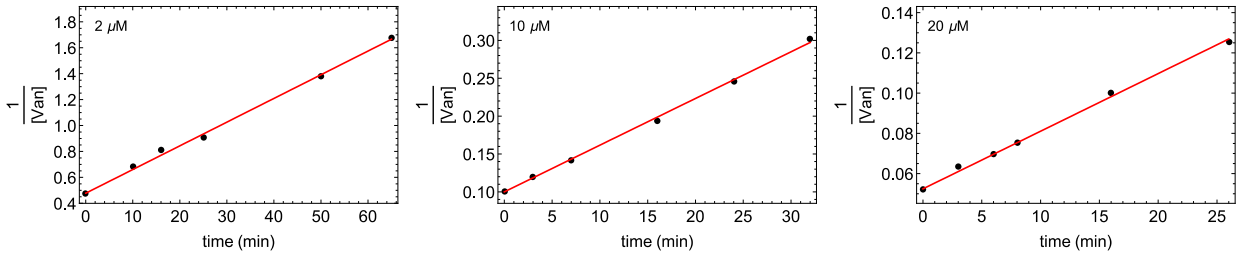

Figure S2. Representative second order fits for photochemical loss of vanillin. All experiments shown are for 310 nm excitation in aqueous solution with pH = 2.

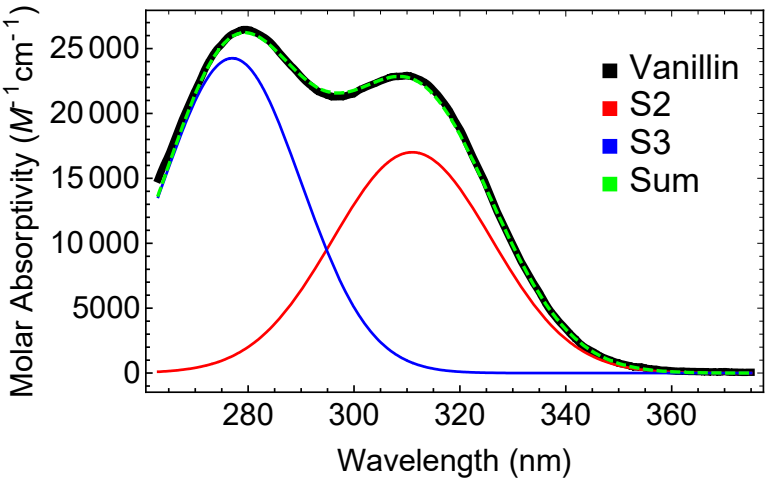

Figure S3. Decomposition of the vanillin UV spectrum (base-e, black) into separate states approximated by Gaussian spectral profiles (S2, blue and S3, red) and the sum of the individual spectra (green). The centers of the individual bands are at 277 nm and 311 nm.

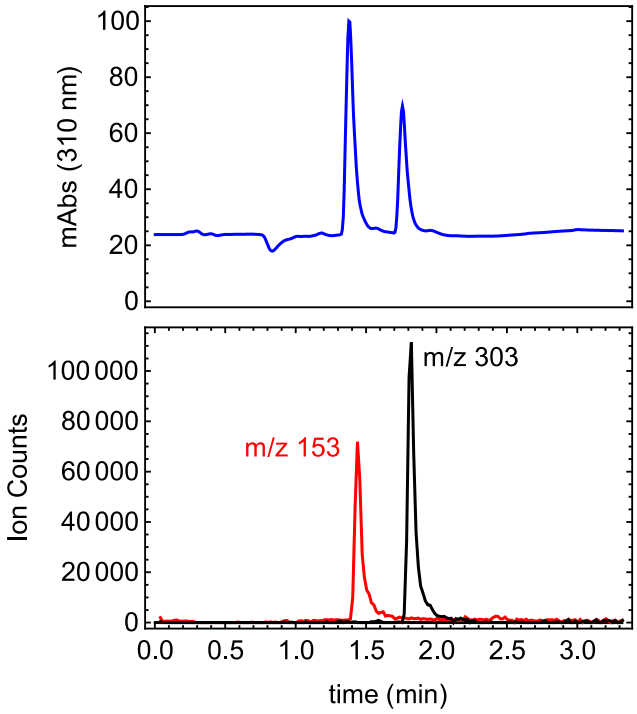

Figure S4. Representative chromatograms for irradiation of 25 μM vanillin at ~50% loss. Top : UV absorbance at 310 nm. Bottom : signal for $M + H^+$ *for vanillin (t_R =1.5 min, m/z 153) and the dimer product (t_R =1.9 min, m/z 303)*

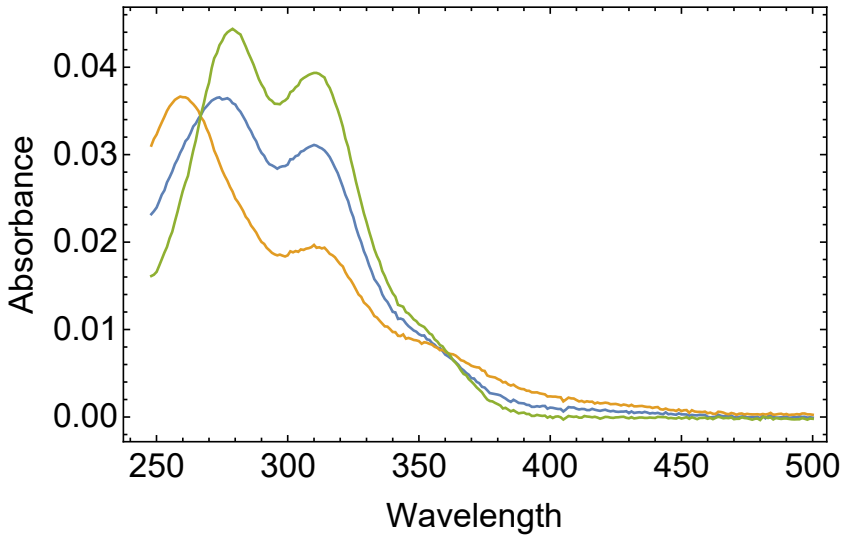

Figure S5. UV Spectra during several time points during the irradiation of 5 uM vanillin with a 310 nm LED. Isosbestic points are present at 355nm and 252nm, indicating predominance of a single product with significant UV absorbance.

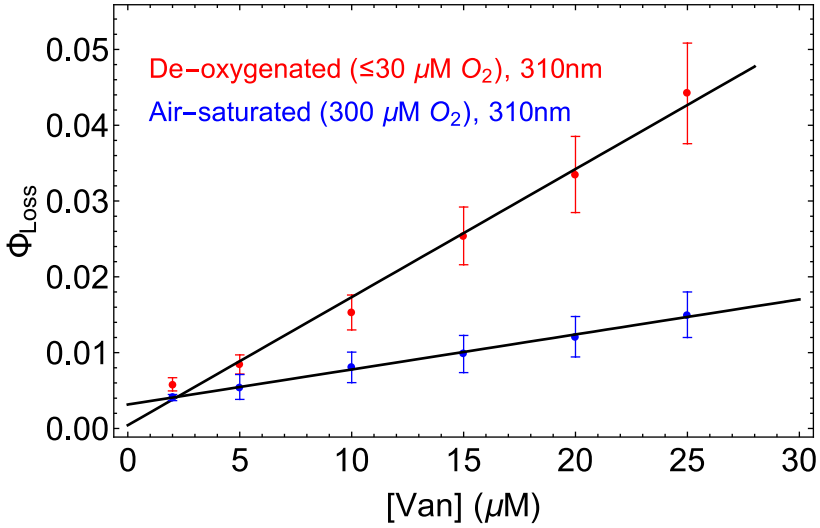

Figure S6. Φ_{loss} *as function of initial [Van] with 310 nm irradiation at pH = 2 with de-oxygenated solution (red) and air-saturated solution (blue).*

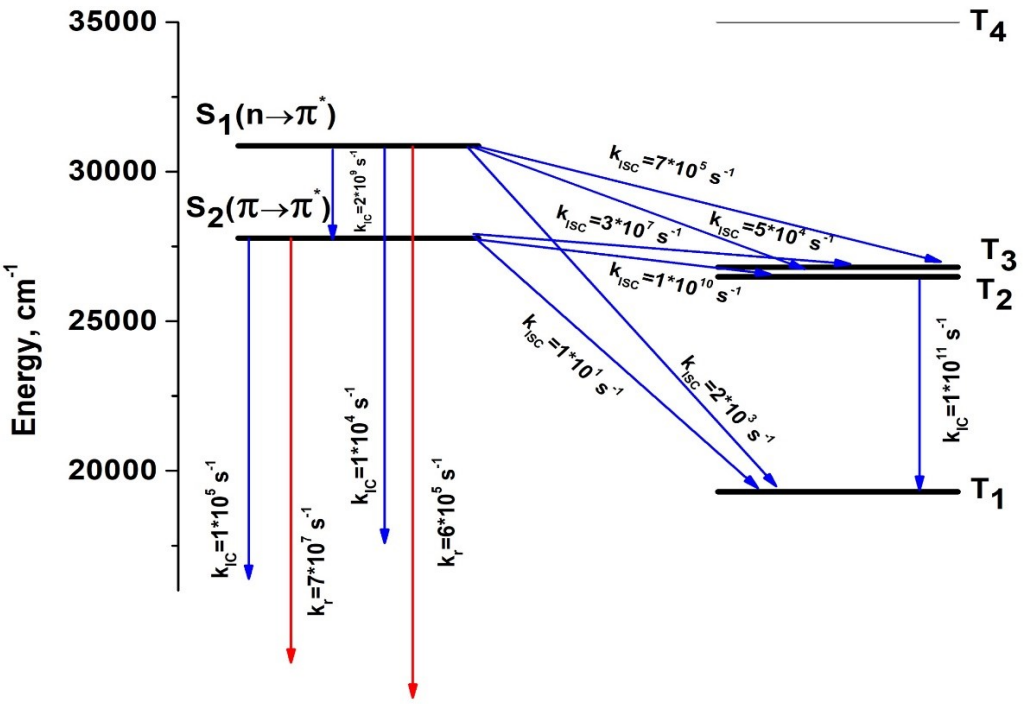

Figure S7. The Jablonski diagram for vanillin in water, at the S_2 equilibrium geometry. Note that after vibrational relaxation, S_2 becomes the lowest energy excited state at its equilibrium geometry. The k_r are radiative rate constants, k_{ISC} are intersystem crossing rate constants and k_{IC} are internal conversion rate constants.

Supplemental Tables

Table S1. The computed wavelengths in nm of electronic transitions and oscillator strengths (*f*) in parenthesis for vanillin+h_2o using PCM/TDDFT/B3LYP/6-31G** in the S_0 and S_2 geometries. The electronic natures of transitions are given as well.

S_0 geometry	
Transition	Wavelength (*f*)
$S_0 \rightarrow S_1$	308 (0.0003) n→π*
$S_0 \rightarrow S_2$	304 (0.17) π→π*
$S_0 \rightarrow S_3$	268 (0.22) π→π*
S_2 geometry	
$S_0 \rightarrow S_2$	360.25 (0.22) π→π*
$S_0 \rightarrow S_1$	324.36(0.0004) n→π*
$S_0 \rightarrow S_3$	285.8(0.33) π→π*

Table S2. Ratio of the lifetimes for photochemical loss of vanillin assuming a single, given SZA and at specific latitudes on the dates of the solstice and equinox. The lifetimes have been multiplied by the ratio of solar intensities to remove the dependence on photon flux and emphasize the dependence on the variation on the solar spectrum rather than its intensity. Values in parentheses are $\frac{\tau_{min,lat}}{\tau_{SZA}}$ and do not account for the difference in the peak solar flux at a given latitude and the chosen/reported SZA.

$\frac{\tau_{min,lat}}{\tau_{SZA}} * \frac{I_{solar,max,lat}}{I_{solar,SZA}}$	$SZA = 0^\circ$		$SZA = 45^\circ$		$SZA = 60^\circ$	
	$15^\circ N$	$45^\circ N$	$15^\circ N$	$45^\circ N$	$15^\circ N$	$45^\circ N$
Summer Solstice	1.0 (1.0)	1.0 (1.1)	0.9 (0.6)	0.9 (0.7)	0.8 (0.4)	0.8 (0.4)
Equinox (Fall/Spr)	1.0 (1.2)	1.1 (1.6)	0.9 (0.8)	1.0 (1.0)	0.8 (0.4)	0.9 (0.6)
Winter Solstice	1.1 (2.1)	1.5 (4.8)	1.0 (1.3)	1.3 (3.0)	0.8 (0.8)	1.2 (1.7)

Supplemental Text

S1. Excited State Dynamic Calculations

Within the Franck-Condon approximation, and using linear coupled model (the hessians of initial (S_i) and final electronic (T_j) states are assumed to be equal), the $k_{ISC-TD}(S_i \rightarrow T_j)$ rate can be calculated as [14]

$$k_{ISC-TD}(S_i \rightarrow T_j) = \frac{\langle \Psi(S_i) | \hat{H}_{SO} | \Psi(T_j) \rangle^2}{\hbar^2} \int_{-\infty}^{\infty} e^{\Phi(t)} dt \quad \text{(S1)}$$

Here, $\Phi(t) = \frac{i}{\hbar}\Delta E t + y_\mu \left(e^{i\omega_\mu t} - 1 \right) + 2 y_\mu m_\mu (1 - cos(\omega_\mu t))$ and $m_\mu = \frac{1}{1 - e^{\frac{\hbar\omega}{kt}}}$ is the Boltzmann population of the μ-th mode vibrational level with frequency ω_μ. The y_μ is the Huang-Rhys factor related to the equilibrium position displacement of the μ-th mode during the $S_i \rightarrow T_j$ transition, with an adiabatic energy gap ΔE. The integral (X1) is calculated using the saddle point method [14]:

$$k_{ISC-TD}(S_i \rightarrow T_j) = \sqrt{\frac{2\pi}{|\Phi''(\tau_T)|}} \cdot e^{\Phi(\tau_T)} \frac{\langle \Psi(S_i) | \hat{H}_{SO} | \Psi(T_j) \rangle^2}{\hbar^2} \quad \text{(S2)}$$

Here, the second derivative of $\Phi(t)$ is

$$\Phi''(t) = -y_\mu \omega_\mu^2 (e^{i\omega_\mu t} + 2 m_\mu ch(\omega_\mu t)) \quad \text{(S3).}$$

The first saddle point (τ_T) can be found by solving following expression [14]:

$$\hbar\omega_\mu y_\mu \left(e^{i\omega_\mu \tau_T} + 2 m_\mu sh(\omega_\mu \tau_T) \right) = \Delta E \quad \text{(S4).}$$

The τ_T and finally $k_{ISC-TD}(S_i \rightarrow T_j)$ depend on the effective temperature (T). T can be connected to the occupancies of vibrational levels, and finally to the vibrational energy of the S_i state [14].

S2. Screening Effects

Due to absorption by the sample, the solution closer to the illumination source (at the bottom of the quartz vial) will receive a larger photon flux than the solution further from the illumination

source (at the top of the liquid level). In effect, the photochemical reaction necessarily proceeds faster in the solution at the bottom of the vial than the solution at the top of the vial. To account for this, the light absorption weighted internal screening factor, S, is calculated. S is the ratio of the actual fraction of light absorbed compared to the fraction of light absorbed under optically thin conditions. All calculated quantum yields are divided by S, to account for an artificially slower volume-averaged reaction rate in solutions that are optically thicker (e.g. larger volume or higher concentration).

$$S = \frac{\sum\left(1 - 10^{-\varepsilon * l * [Van]}\right)}{\sum 2.303 * \varepsilon * l * [Van]} \tag{6}$$

S3. Effects of Oxygenation Levels

The values of k_{SR} and Φ_1 can be estimated for both air-saturated and de-oxygenated conditions. The fundamental processes described by these rate constants are not different in air-saturated or deoxygenated conditions, yet secondary chemistry in the presence of oxygen complicates the direct relation between the two cases. Differences in k_{SR} and Φ_1 values with varying $[O_2]$ will indicate the importance of quenching, regeneration of vanillin, and production of secondary radical species. With an upper limit of $[O_2] = 30\ \mu M$ in our deoxygenated experiments, $k_1 = 1.56 * 10^5 s^{-1}$. Under deoxygenated conditions, Φ_{Loss} are much higher in the presence of oxygen within the measured concentration range, as expected in the absence of this bimolecular quenching process.